Image Compression by SPIHT Coding using Traditional Wavelets

[1]Jaya Krishna Sunkara, [2]K Subramanyam, [3]V. V. Satyanarayana Tallapragada, [4]V Kiran Kumar
[1]Asst. Prof., [2]Asst. Prof. (GKCE), [3]Asso. Prof.(SVEC), [4]Asst. Prof.(PDCE)
[1]Department of ECE,
[1]Sree Vidyanikethan Engineering College (AUTONOMOUS), Tirupati, India

Abstract : Image compression deals with the task of reducing the size of the image without losing the visual quality of the image. Image compression has a number of applications as compression eases the task of storage and transfer of image data. The applications include medical, biometric, remote sensing, mailing services, web page maintenance, etc. The key steps in image compression are image transformation and coding. The different transformations include discrete sine, discrete cosine, haar, walsh, slant, KL, SVD and wavelet transforms. Image coding was done using different coding techniques including Arithmetic coding, Huffman coding, Block truncation coding, vector quantization, embedded zerotree wavelet coding (EZW) and set partitioning in hierarchical trees (SPIHT). Wavelet based transformations and lifting based wavelet transformations are found to be best transformation techniques. The coding techniques EZW and SPIHT are specially designed to operate on wavelet domain of image. These coding techniques, particularly, SPIHT coding was proved to be the best of state of art coding techniques. The JPEG2000 compression standard is well known compression standard accepted worldwide. The JPEG2000 compression standard has utilized the lifting based wavelets cdf5.3, cdf9.7. The JPEG2000 compression standard was originally designed for photographic images. Hence the performance of the JPEG2000 is not the optimum for other image classes like medical images, scanned documents, biometric images, satellite images, 3D (stereoscopy) images, etc. Hence in this research the goal is to devise new compression standard to compress a wide category of image classes. In this paper compression of different kinds of image was considered. The coding technique considered is SPIHT and transformation was done by different traditional wavelets.

Index Terms **- biometric, scanned docs, SPIHT, wavelet.**

I. INTRODUCTION

For a 1-D wavelet transform, a vector of the wavelet coefficients can be divided into subbands after the wavelet decomposition as shown in the figure 1. Similarly, a block of the two-dimensional wavelet coefficients can be divided into subbands as shown in figure 2. An EZW encoder was specially designed by Shapiro [1] to use with wavelet transforms. In fact, EZW coding is more like a quantization method. It was originally designed to operate on images (2D-signals), but it can also be used on other dimensional signals. The EZW encoder is based on progressive encoding to compress an image into a bit stream with increasing accuracy.

The SPIHT coder [2], [3] is a highly refined version of EZW algorithm and is a powerful image compression algorithm that produces an embedded bit stream from which the best reconstructed images in the mean square error sense can be extracted at various bit rates. Some of the best results – highest PSNR values for given compression ratios – for a wide variety of images have been obtained with SPIHT. Hence it has become the benchmark state of the art algorithm for image compression [4].

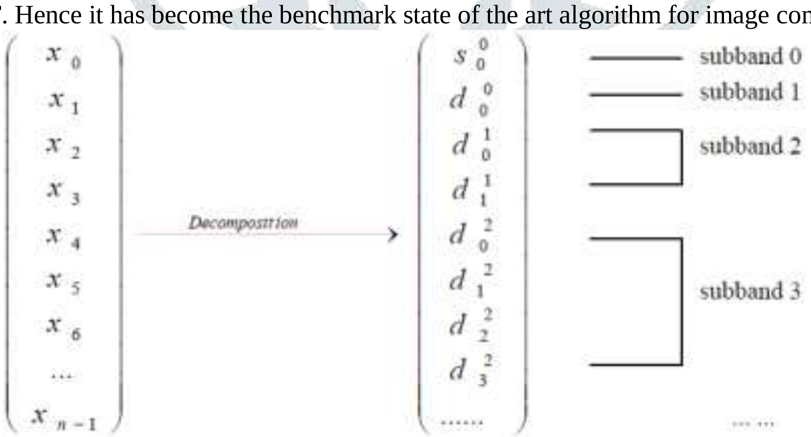

Fig 1: Subbands after the 1-D Wavelet Decomposition

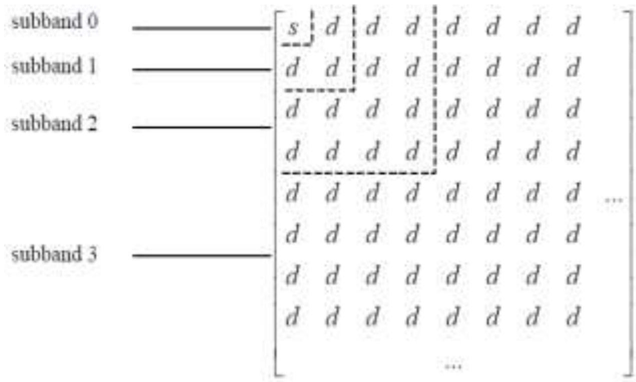

Subband Index	Coefficients Numbers
0	1
1	3
2	12
3	48
...	...

Fig 2: Subbands in a Wavelet Transform Block after the 2-D Wavelet

II. Set Partitioning in Hierarchical Trees (SPIHT) Coding Algorithm

Set partitioning in Hierarchical Trees (SPIHT) is in principle similar to embedded zero tree wavelet (EZW) but the crucial differences being the way the coefficients are partitioned and how the significant information is conveyed to the decoder [5]. The SPIHT algorithm can briefly be outlined as set partitioning sorting algorithm and spatial orientation trees.

a. Set partitioning sorting Algorithm

One important fact used in the design of the sorting algorithm is that no need to sort all coefficients. Actually, an algorithm that simply selects the coefficients such that $2^n \leq C_{i,j} < 2^{n+1}$, with |'n'| decremented in each pass is needed. Given n if $|C_{i,j}| \geq 2^{n+1}$ then a coefficient is significant, otherwise it is called insignificant. The sorting algorithm divides the set of pixels into partitioning subsets T_m and performs the magnitude test.

If the decoder receives a no to that answer (the subset is insignificant), then it knows that all coefficients in T_m, are insignificant. If the answer is yes (the subset is significant), then a certain rule shared by the encoder and the decoder is used to partition T_m, into new subsets T_m and the significance test is then applied to the new subsets. To make clear relationship between magnitude comparisons and message bits, use the function

S_n (T) =1; Max $\{|C_{i,j}|\} \geq 2^n$

0; otherwise

to indicate the significance of a set of coordinates T. To simplify the notation of single pixel sets, write $S_n(\{I,j)\})$ as $S_n(I,j)$.

b. Spatial Orientation Trees

The following sets of coordinates are used to present the new coding method.

0(I,j): set of coordinates of all offspring of node (I,j);

D(I,j): set of coordinates of all descendants of the node;

H : set of coordinates of all spatial orientation tree roots (nodes in the highest pyramid level);

L(I,j) = D(I,j) – O(I,j).

For instance, except at the highest and lowest pyramid levels,

O(I,j) = {(2i,2j), (2i,2j+1), (2i+1,2j),(2i+1,2j+1)}

Use parts of the spatial orientation trees as the partitioning subsets in the sorting algorithm. The set partition rules are simply the following.

1. The initial partition is formed with the sets ((I,j)) and D(I, j) for all (I,j) Є H.
2. IF D(I,j) is significant, then it is partitioned into L (I,j) plus the four single element sets with (K,I) Є O(I, j).
3. If L (I, j) is significant, then it is partitioned into the four sets D(K,I) with (K,I) Є O(I,j).

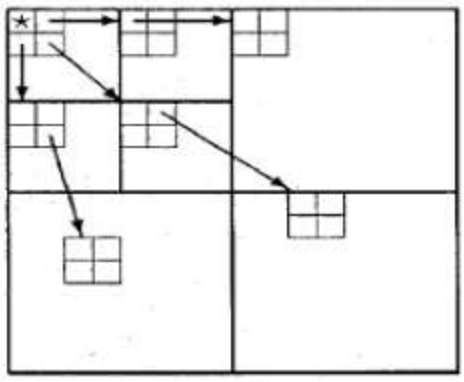

Fig 3: Examples of parent offspring dependencies in the spatial orientation tree

c. Important Features of SPIHT

- Good image quality, high PSNR and low MSE.
- Produces a fully embedded coded file.
- Fast coding/decoding algorithm.
- It can code with exact bit rate or distortion.

- Efficient combination with error protection.
- It is optimized for progressive image transmission.
- The SPIHT coder is also a highly refined version of EZW algorithm and is a powerful image compression algorithm.
- Bit level compression.

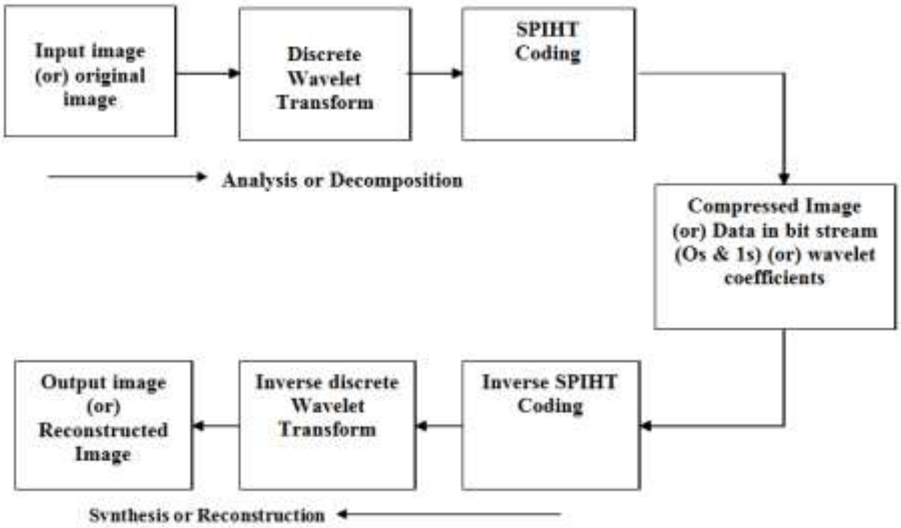

Fig 4: Block diagram of encoder & decoder part of SPIHT algorithm.

The following steps are involved in the compression algorithm of discrete wavelet Transform (DWT).

1. Read the input image (Color/Monochrome).
2. Apply forward DWT.
3. Obtain cutoff value based on given percentage of coefficients to be retained.
4. Set small coefficients to zero.
5. Apply inverse DWT to the result of Step 4.

III. CLASSICAL WAVELETS

The Fourier analysis is based on decomposing a function per sine waves with different frequencies. Similarly, the wavelet analysis is the decomposition of a function onto shifted and scaled versions of the basic wavelet. A wavelet is a wave shaped function having a limited length with a zero mean value. This means that a wavelet decreases fast enough in the frequency domain, and that

$$\hat{\psi}(0) = \int \psi(x)dx = 0$$

which is a consequence of the condition for the existence of the inverse wavelet transform. Unlike a sine wave, wavelets are generally irregular and asymmetrical.

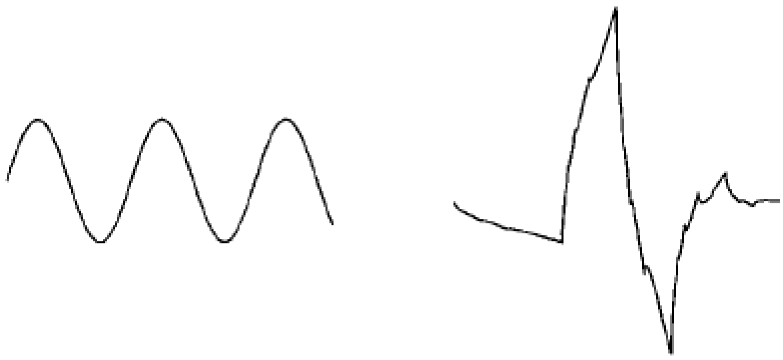

Fig 5: Sine function and a wavelet

It is intuitively clear that functions with sharp changes can be analyzed better using short irregular waves than with a smooth infinite sine. The wavelet basis $\{\psi_{j,k}(x)\}_{j,k}$ is generated by the translation and dilatation $\psi(2^{-j} x - k)$ of the basic ("mother") wavelet $\psi(x)$. If the basic wavelet $\psi(x)$ ($\psi(x) \equiv \psi_{0,0}(x)$) starts at the moment of x = 0 and ends at the moment of x = N - 1, the shifted wavelet $\psi_{o,k}$ starts at the moment of $x = k$ and ends at the moment of $x = k + N - 1$. The scaled wavelet $\psi_{j,0}$ starts at the moment of $x = 0$ and ends at the moment of $x = 2^j (N - 1)$. Its graph is scaled (compressed or expanded, depending of the sign of j) by a factor of 2^{-j}, while the graph of the wavelet $\psi_{0,k}$ is translated to the right by k, if $k > 0$,

Scaling $\psi_{j,0}(x) = 2^{-j/2}\, \psi(2^{-j}x)$,

Translation $\psi_{0,k}(x) = \psi(x - k)$.

The basis wavelet is generated by scaling the basic wavelet j times and shifting it by k,

$$\psi_{j,k}(x) = 2^{-j/2}\, \psi(2^{-j} x - k)$$

The multiplier $2^{-j/2}$ is a normalizing factor, so that the L_2 norm of the wavelet is equal to one. The space of details on the j-th resolution level *Wj* contains functions that are linear combinations of wavelets $\psi_{j,k}(x)$.

1-D Continuous wavelet transform

The 1-D continuous wavelet transform is given by:

$$W_f(a, b) = \int_{-\infty}^{\infty} x(t)\psi_{a,b}(t)dt$$

The inverse 1-D wavelet transform is given by:

$$x(t) = \frac{1}{C}\int_{a=0}^{\infty}\int_{b=-\infty}^{\infty} W_f(a,b)\psi_{a,b}(t)db\frac{da}{a^2}$$

where $$C = \int_{-\infty}^{\infty}\frac{|\psi\omega)|^2}{\omega}d\omega < \infty$$

$\Psi(\omega)$ is the Fourier transform of the mother wavelet $\Psi(t)$. *C* is required to be finite, which leads to one of the required properties of a mother wavelet. Since *C* must be finite, then $\Psi(0) = 0$ to avoid a singularity in the integral, and thus the $\Psi(t)$ must have zero mean. This condition can be stated as $\int_{-\infty}^{\infty}\psi(t)dt = 0$ and known as the admissibility condition.

2-D Discrete wavelet transform

The 1-D DWT can be extended to 2-D transform using separable wavelet filters. With separable filters, applying a 1-D transform to all the rows of the input and then repeating on all of the columns can compute the 2-D transform. When one-level 2-D DWT is applied to an image, four transform coefficient sets are created. As depicted in figure 6 (c), the four sets are LL, HL, LH, and HH, where the first letter corresponds to applying either a low pass or high pass filter to the rows, and the second letter refers to the filter applied to the columns.

The Two-Dimensional DWT (2D-DWT) converts images from spatial domain to frequency domain. At each level of the wavelet decomposition, each column of an image is first transformed using a 1D vertical analysis filter-bank. The same filter-bank is then applied horizontally to each row of the filtered and subsampled data. One-level of wavelet decomposition produces four filtered and subsampled images, referred to as subbands.

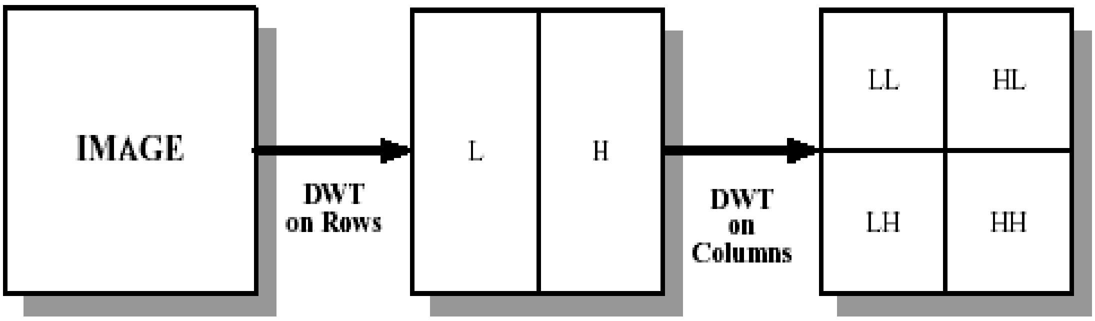

Fig 6: Block Diagram of DWT (a) Original Image (b) Output image after the 1-D applied on Row input (c) Output image after the second 1-D applied on row input

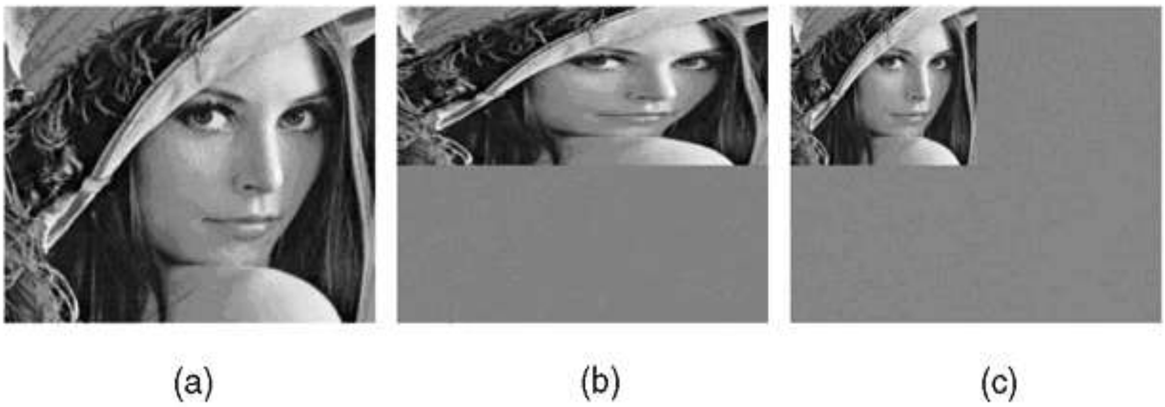

Fig 7: DWT for Lena image (a) Original Image (b) Output image after the 1-D applied on column input (c) Output image after the second 1-D applied on row input

The upper and lower areas of figure 7(b), respectively, represent the low pass and high pass coefficients after vertical 1D-DWT and subsampling. The result of the horizontal 1D-DWT and subsampling to form a 2D-DWT output image is shown in figure 7(c). Multiple levels of wavelet transforms can be used to concentrate data energy in the lowest sampled bands. Specifically, the LL subband in Figure 6(c) can be transformed again to form LL2, HL2, LH2, and HH2 subbands, producing a two-level wavelet transform.

An (R-1) level wavelet decomposition is associated with R resolution levels numbered from 0 to (R-1), with 0 and (R-1) corresponding to the coarsest and finest resolutions. The straight forward convolution implementation of 1D-DWT requires a large amount of memory and large computation complexity. An alternative implementation of the 1D-DWT, known as the lifting scheme, provides significant reduction in the memory and the computation complexity. Lifting also allows in-place computation of the wavelet coefficients. Nevertheless, the lifting approach computes the same coefficients as the direct filter-bank convolution. To employ wavelets for image decomposition is replaced with the notion of "time", which has heretofore served as our free variable, with "spatial position". In addition the wavelet framework has to deal with the two-dimensional signals. Although two-dimensional wavelets can be constructed, a more popular approach is to transform images using one-dimensional *separable wavelets* as suggested by Mallat [6], Antonini *et al*. [7] and [8]-[12]. A number of compression schemes were devised using wavelets. Both image and video compression schemes were devised [13]-[17]. Using separable wavelets means that one can apply the wavelet transform first in a direction and then transform the result again in the other direction. In figure 4 first apply DWT to every row (x-direction) of an image, relocating the scaling coefficients to the left side and the wavelet coefficients to the right side as before. Afterwards apply DWT in the y-direction on the resulting image, relocated scaling coefficients to the top.

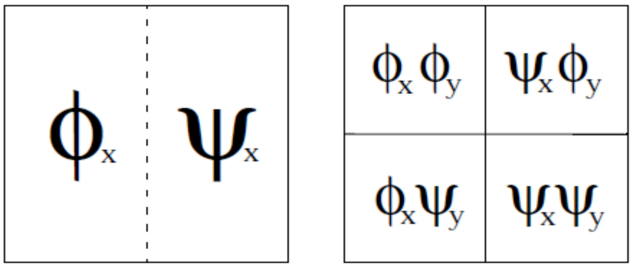

Fig 8: Two-dimensional transform with separable wavelets

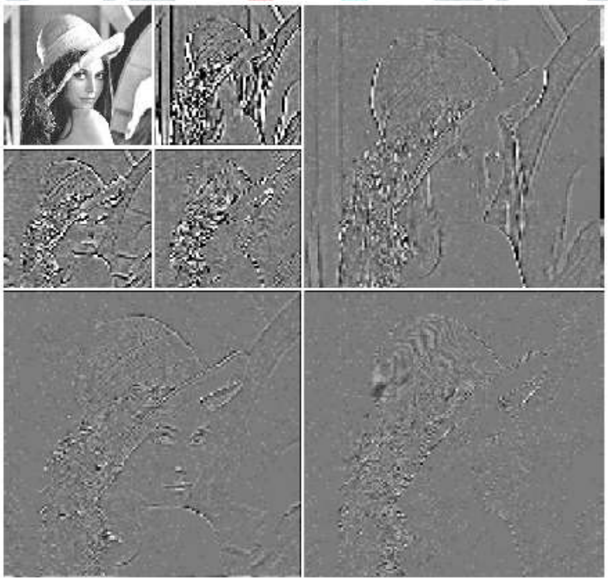

Fig 9: 2-level decomposition of LENA image

Different filter banks can be used for each direction if desired. The upper left quadrant will, after both transformations, contain the original image at half of the resolution, while the other quadrants contain the refinement coefficients necessary to bring the smaller image back to full scale. Each of the quadrants have their own basis functions, thus the basis for separable 2D-transforms consists of one scaling function Φ_x Φ_y and three wavelet functions $\Psi_x\Phi_y$, $\Phi_x\Psi_y$ and $\Psi_x\Psi_y$. After executing DWT in both directions, the algorithm can be recursively applied to the lower resolution image. Figure 9 shows the wavelet coefficients of LENA after 2 levels of decomposition with Daubechies 4-tap wavelet. Recognize the original image in the upper left, now scaled down to 25% resolution. The wavelet coefficients, especially those from level 1, are so small that they are almost imperceptible (the gray-levels have been contrast enhanced for improved viewing).

This illustrates the efficiency of wavelet transforms for energy compaction. Interestingly (and quite unlike the Fourier transform) the wavelet coefficient quadrants visually resemble the high-resolution details of the image. The lower left quadrant has mostly details for the x-direction, while the upper right has details for the y-direction. The lower right quadrant has details from both directions (diagonal) but they are almost too fine to see. (The other two wavelet quadrants paint in broader strokes because their bases contain a scaling function). The actual compression is accomplished by discarding coefficients. For instance, discard some of the quadrants in the decomposition, but a better strategy would be to selectively discard coefficients based on their magnitude. Since larger coefficients probably have more impact on the reconstructed image, keep those and rather discard the smaller values. This is known as *thresholding*. With "hard thresholding" a tolerance limit *T* should be selected and discard all coefficients with absolute value smaller than *T*. A variation on this scheme is called "quantile thresholding" in which a percentage *P* will be selected and smallest *P* percent of the values will be discarded. With "soft thresholding" the magnitude of all coefficients are reduced by the amount *T*.

(a) (b) (c)

Fig 10: Lena image compressed with Daubechis 4-tap wavelet. (a) Original (left), (b) 80% compressed image and (c) 96% compressed image

The coefficients that are smaller than this value are reduced to zero while all the rest are brought closer to zero. Instead of subtraction, also, use of integer division by *Q* is followed. Again, all values smaller *Q* than would be reduced to zero, while the rest are made smaller. This strategy would also limit the number of different values for coefficients, which in effect could make coding more efficient, since the number of bits required to code the values can be reduced. The process of limiting the set of possible values used is known as *quantization*. An even more advanced approach is to use different values of *T* or *Q* for different subbands. Since the human visual system is less sensitive to high frequencies, for instance use a greater threshold-value or a coarser quantization for the fine-detail subbands. An example of wavelet compression is shown in figure 10.

In the middle picture the smallest 80% of the wavelet coefficients have been discarded before reconstructing the image (hard threshold). At this compression level there is no perceivable reduction in image quality. The only visual effect seems to be a reduction of noise and a slight smoothing of texture. The rightmost picture is reconstructed from only 4% of the original coefficients. The image is now composed of 2621 wavelets of different sizes and positions, as compared to 65536 pixels in standard representation. Compression artifacts have now become apparent, but even at this high level of compression the image is quite recognizable. In comparison, a JPEG representation at this compression level would on average synthesize each patch of only 2.5 basis patterns.

IV. Basis Functions of Traditional Wavelets

a. Haar

Any discussion of wavelets begins with Haar wavelet, the first and simplest. Haar wavelet is discontinuous, and resembles a step function. It represents the same wavelet as Daubechies db1. The basis function of Haar wavelet is shown in figure 11.

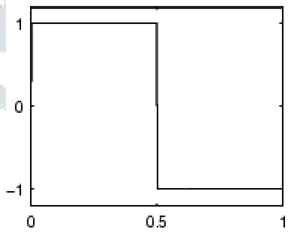

Fig 11: Basis function of Haar Wavelet

b. Daubechies

Ingrid Daubechies, one of the brightest stars in the world of wavelet research, invented what are called compactly supported orthonormal wavelets -- thus making discrete wavelet analysis practicable. The names of the Daubechies family wavelets are written dbN, where N is the order, and db the "surname" of the wavelet. The db1 wavelet, as mentioned above, is the same as Haar wavelet. The figure 12 shows the wavelet functions of the next nine members of the family.

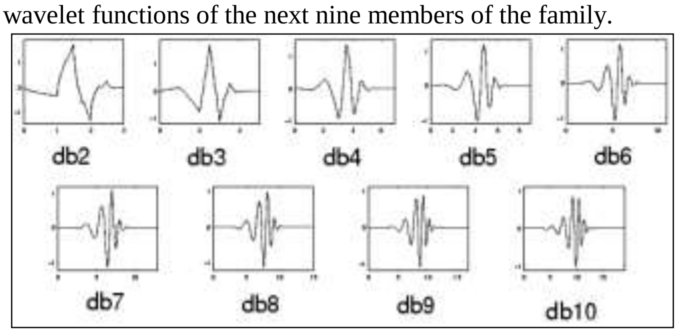

Fig 12: Basis functions of Daubechies Wavelet Family

c. Biorthogonal

This family of wavelets exhibits the property of linear phase, which is needed for signal and image reconstruction. By using two wavelets, one for decomposition (on the left side) and the other for reconstruction (on the right side) instead of the same single one, interesting properties are derived. The basis functions of Biorthogonal wavelets are shown in figure 13.

d. Coiflet

Coiflet wavelets are built by I. Daubechies on the request of R. Coifman. The wavelet function has 2N moments equal to 0 and the scaling function has 2N-1 moments equal to 0. The two functions have a support of length 6N-1. The figure 14 shows the basis functions of the family of Coiflet wavelets.

e. Symlet

The symlets are nearly symmetrical wavelets proposed by Daubechies as modifications to the db family. The properties of the two wavelet families are similar. The figure 15 shows the wavelet functions.

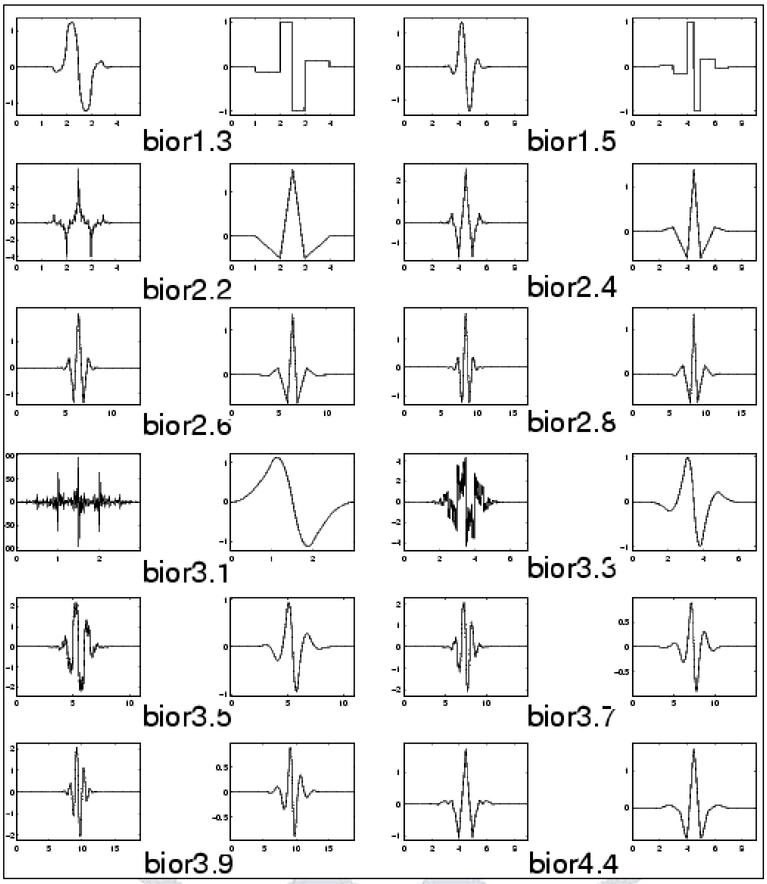

Fig 13: Basis functions of Bi-orthogonal Wavelet Family

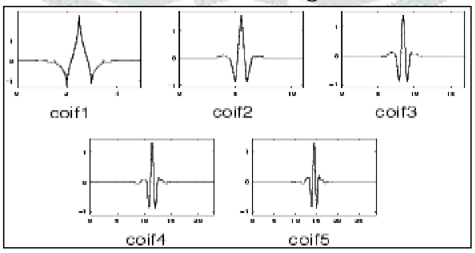

Fig 14: Basis functions of Coiflet Family

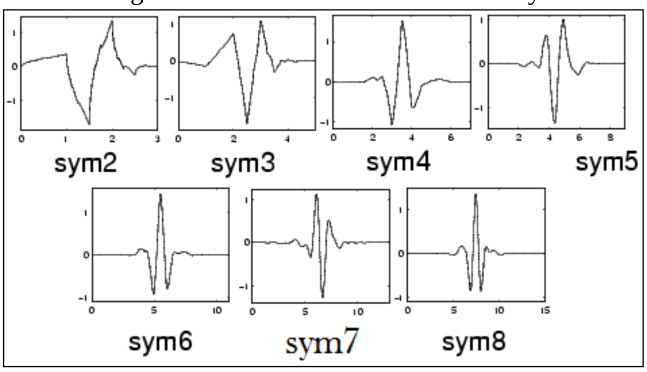

Fig 15: Basis functions of Symlet Family

f. Di-Meyer

The Meyer wavelet and scaling function are defined in the frequency domain. The discrete version of Meyer wavelet is usually written as Di-meyer of which the basis function is plotted in the figure 16.

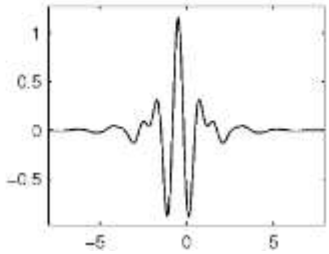

Fig 16: Basis function of Discrete Meyer Wavelet

V. SIMULATION RESULTS

In this section simulation results of compression of different kinds of images are presented. The image category includes biometric images, medical images, scanned documents, satellite images and 3D images. The biometric images are useful for verification of individuals in different applications. The thumb print images are useful in identifying the criminals. The biometric images are used in authenticating people in offices, colleges and many institutions. Usually it requires the storage of large set of images. Hence the compression of these images is crucial. Medical images are useful in treatment of different anomalies. The transfer and storage of these images plays an important role in modern medical institutes. Scanned documents from fax machines, scanners, phone scanners are common in the current era, and the compression of the documents is important. Satellite images contains images of earth surfaces, ocean waves, space phenomena. These images are usually processed by scaling them according to the capturing element characteristics. 3D images includes the depth axis logically but physically these are 2D images only. The size of the 3D and satellite images is high. Tables 1 to 5 gives the performance of SPIHT and traditional wavelets on biometric, medical, scanned, satellite and 3D images respectively. The figure 16 to 22.

TABLE I: Performance results of Compression of Biometric images using different wavelets with SPIHT

Performance results of Compression of Biometric images using different wavelets with SPIHT										
	Thumb Print – 1		**Thumb Print – 2**		**Iris – 1**		**Iris – 2**		**Retina**	
	CR	**PSNR**	**CR**	**PSNR**	**CR**	**PSNR**	**CR**	**PSNR**	**CR**	**PSNR**
Haar	2.1	29.96	2.25	29.95	2.41	36.77	2.33	36.59	2.85	39.25
db5	1.97	29.73	2.08	29.91	2.29	37.37	2.18	36.86	2.72	35.2
bior 1.3	1.93	15.44	2.07	15.76	2.2	33.81	2.13	31.13	2.58	33.71
coif5	1.76	21.99	1.87	19.38	2.01	36.35	1.91	34.3	2.4	35.24
sym8	1.9	23.95	2.01	21.85	2.19	36.82	2.08	35.46	2.63	35.24
Dmey	1.13	22.6	1.22	19.82	1.29	36.43	1.21	34.4	1.54	35.27

TABLE II: Performance results of Compression of Medical images using different wavelets with SPIHT

Performance results of Compression of Medical images using different wavelets with SPIHT										
	Image – 1		**Image -2**		**Image -3**		**Image -4**		**Image -5**	
	CR	**PSNR**	**CR**	**PSNR**	**CR**	**PSNR**	**CR**	**PSNR**	**CR**	**PSNR**
Haar	2.69	38.19	2.14	36.09	2.63	37.4	2.68	38.84	2.93	38.87
db5	2.75	38.53	2.06	36.38	2.52	33.4	2.54	34.01	2.75	33.78
bior 1.3	2.61	36.56	1.97	25.49	2.39	26.33	2.42	24.48	2.65	24.41
coif5	2.42	37.87	1.81	31.44	2.25	32.21	2.22	31.43	2.42	30.85
sym8	2.63	38.13	1.98	33.04	2.44	32.82	2.43	32.81	2.63	32.97
Dmey	1.58	37.94	1.15	31.82	1.44	32.3	1.4	32.67	1.51	31.41

TABLE III: Performance results of Compression of Scanned doc images using different wavelets with SPIHT

Performance results of Compression of Scanned document images using different wavelets with SPIHT										
	Image - 1		**Image -2**		**Image -3**		**Image -4**		**Image -5**	
	CR	**PSNR**	**CR**	**PSNR**	**CR**	**PSNR**	**CR**	**PSNR**	**CR**	**PSNR**
Haar	3.04	39.68	2.6	37.22	2.88	42.89	2.38	30.27	2.53	36.98
db5	2.85	38.37	2.39	37.29	2.86	42.44	2.04	29.9	2.24	36.55

bior 1.3	2.96	32.43	2.37	28.42	2.82	38.15	2.15	19.02	2.31	26.5
coif5	2.54	32.32	2.11	31.64	2.49	40.06	1.81	21.21	1.96	29.88
sym8	2.73	34.36	2.29	33.97	2.74	41.09	1.96	23.55	2.14	31.8
Dmey	1.57	32.54	1.35	29.85	1.58	40.13	1.17	21.16	1.22	30.15

TABLE IV: Performance results of Compression of Satellite images using different wavelets with SPIHT

Performance results of Compression of Satellite images using different wavelets with SPIHT										
	Image – 1		**Image -2**		**Image -3**		**Image -4**		**Image -5**	
	CR	**PSNR**	**CR**	**PSNR**	**CR**	**PSNR**	**CR**	**PSNR**	**CR**	**PSNR**
Haar	2.18	36.06	2.95	39.11	2.74	38.09	2.85	38.79	2.25	36.4
db5	2.04	36.23	3.29	35.28	2.88	34.55	3.17	34.56	2.05	36.26
bior 1.3	1.99	26.88	2.87	36.5	2.66	37.97	2.56	38.24	2.19	26.11
coif5	1.78	31.76	2.88	35.28	2.77	34.6	2.54	34.61	1.91	39.65
sym8	1.96	33.27	3.16	35.28	3.03	34.61	2.78	34.64	2.09	31.74
Dmey	1.13	31.96	1.84	35.31	1.76	34.61	1.61	34.64	1.23	29.74

TABLE V: Performance results of Compression of 3D images using different wavelets with SPIHT

Performance results of Compression of 3D images using different wavelets with SPIHT										
	Image – 1		**Image -2**		**Image -3**		**Image -4**		**Image -5**	
	CR	**PSNR**	**CR**	**PSNR**	**CR**	**PSNR**	**CR**	**PSNR**	**CR**	**PSNR**
haar	2.13	35.86	2.56	37.82	2.71	38.3	2.85	39.13	2.71	38.51
db5	2.01	36.02	2.76	38.92	2.52	33.06	2.81	39.13	2.53	38.72
bior 1.3	1.95	24.79	2.5	27.1	2.45	29.47	2.78	32.23	2.46	31.81
coif5	1.75	30.88	2.23	35.29	2.19	32.15	2.48	35.95	2.23	35.74
sym8	1.93	32.52	2.66	36.67	2.4	32.69	2.7	37.07	2.43	37.01
dmey	1.12	31.07	1.4	35.57	1.4	32.2	1.6	35.95	1.43	35.86

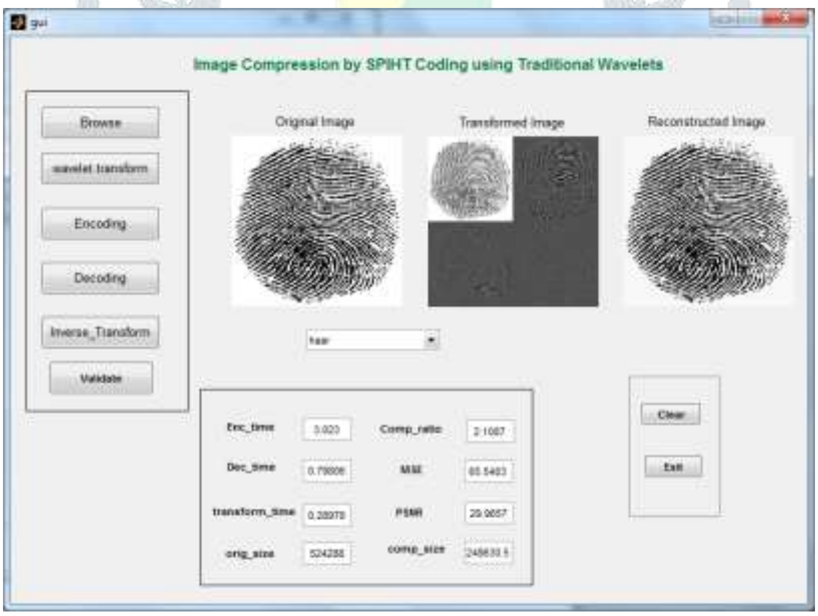

Fig. 16 Screen shot of Compression of Biometric image - 1

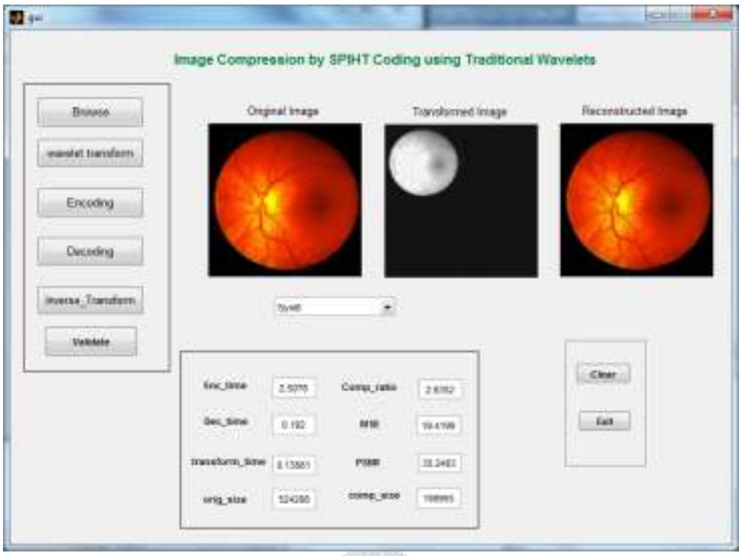

Fig. 17 Screen shot of Compression of Biometric image - 2

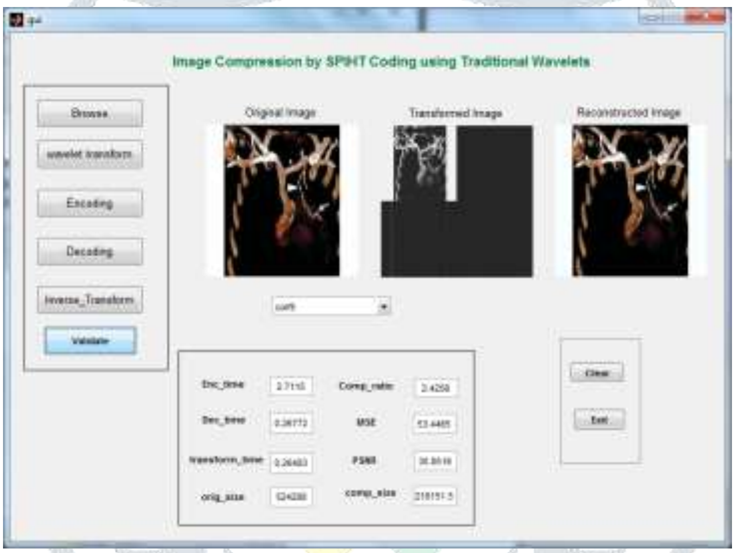

Fig. 18 Screen shot of Compression of Medical image

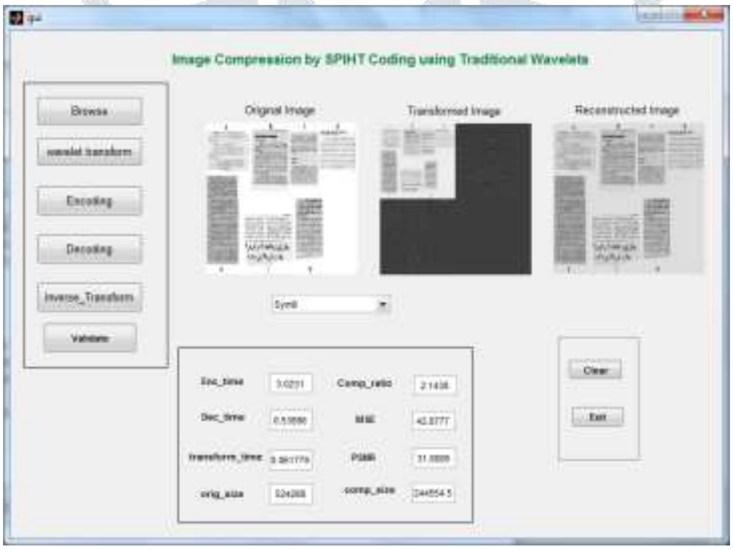

Fig. 19 Screen shot of Compression of Scanned doc imag

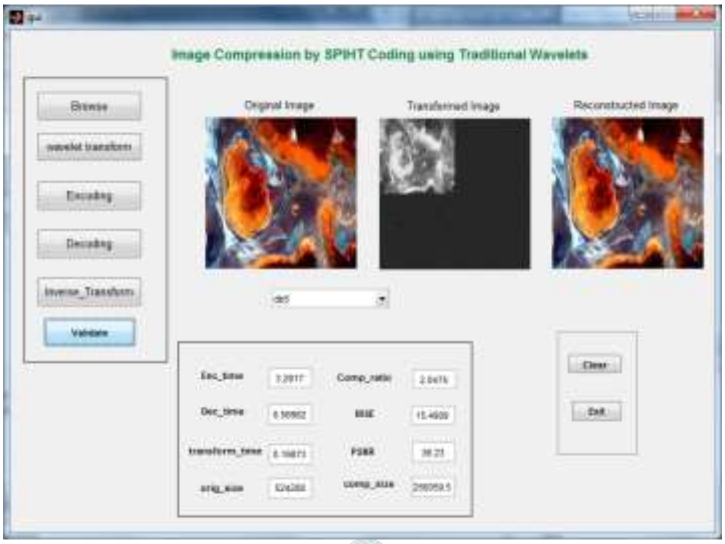

Fig. 20 Screen shot of Compression of Satellite image - 1

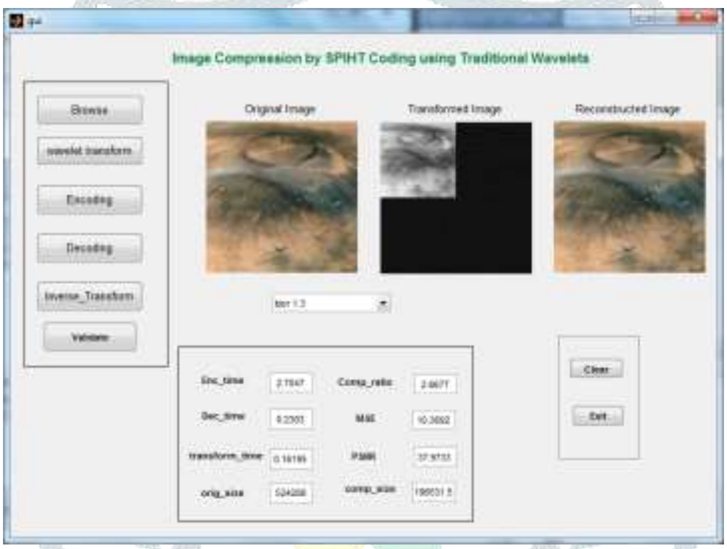

Fig. 21 Screen shot of Compression of Satellite image – 2

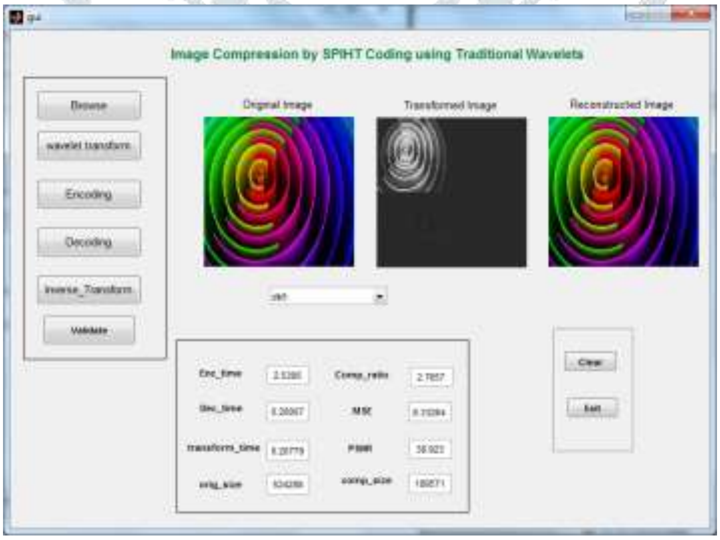

Fig. 22 Screen shot of Compression of 3D image

VI. CONCLUSIONS

In this paper an attempt has been made to compress a wide category of images using traditional wavelets. Biometric, medical, scanned documents, satellite and 3D images are considered. The traditional wavelets haar, daubeuchies, coiflet, symlet and demeyer wavelets are considered. The coding was done by SPIHT coding. A large number of images are considered under each category and results of 5 images under each category is presented in the paper. The performance of the compression scheme is almost similar with all the wavelets except demeyer wavelet. The performance of haar wavelet is better in comparison with that of the other wavelets. The average value of compression ratio with the Biometric, medical, scanned documents, satellite and 3D images are 2.04bpp, 2.26bpp, 2.27bpp, 2.37bpp and 2.25bpp. The average value of peak signal to noise ratio with the Biometric, medical, scanned documents, satellite and 3D images are 30.69dB, 33.41dB, 32.99dB, 34.75dB and 34.58dB. The compression performance is expected to be improved if better transformation and coding techniques are employed.

REFERENCES

[1] J. M. Shapiro. "Embedded Image Coding Using Zero-trees of Wavelet Coefficients", IEEE Transactions on Signal Processing, Vol. 41, No. 12 (1993), pp. 3445-3462.

[2] Amir Said, and Pearlman, W. A. A New, Fast, and Efficient Image Codec Based on Set Partitioning in Hierarchical Trees, IEEE Trans. Circuit and systems for Video Technology, vol. 6, no. 3, June 1996, pp.243-250.

[3] Asad Islam & Pearlman, "An embedded and efficient low-complexity, hierarchical image coder", Visual Communication and Image processing'99proceedings of SPIE., Vol. 3653, Jan1999, pp.294-305.

[4] Strang, G. and Nguyen, T. Wavelets and Filter Banks, Wellesley-Cambridge Press, Wellesley, MA,1996,

[5] Amir Said and William A.Pearlman, 1996, "A new fast and efficient image codec based on set partitioning in hierarchical trees", IEEE Trans. Circuits Systems for video Tech, Vol.6, pp.243-250.

[6] Stephane G. Mallat (1989), "A Theory for Multiresolution Signal Decomposition: The Wavelet Representation", *IEEE Transactions on Pattern Analysis and Machine Intelligence, pp.* 674-693.

[7] M. Antonini, M. Barlaud, P. Mathieu, and I. Daubechies, "Image coding using the wavelet transform," *IEEE Tran. on Image Processing*, vol. 1, no. 2, Apr. 1992, pp.205-220.

[8] Haar, Alfred (1910). "Zur Theorie der orthogonalen Funktionensysteme". *Mathematische Annalen* 69 (3): 331–371. doi:10.1007/BF01456326.

[9] Lee, B.; Tarng, Y. S. (1999). "Application of the discrete wavelet transform to the monitoring of tool failure in end milling using the spindle motor current".

[10] "Orthogonal system". *Encyclopedia of Mathematics*. http://eom.springer.de/O/o070380.htm.

[11] Shen, Gilbert G. (2001). *Wavelets and Other Orthogonal Systems*. Boca Raton: Chapman. ISBN 1584882271.

[12] The Haar Transform, http://sepwww.stanford.edu/public/docs/sep75/ray2/paper_html/node4.html

[13] Jaya Krishna Sunkara, Kuruma Purnima, E Navaneetha Sagari and L Rama Subbareddy, "A New Accordion Based Video Compression Method", i-manager's Journal on Electronics Engineering, vol. 1, No. 4, pp. 14-21, June - August 2011.

[14] Jaya Krishna Sunkara, E Navaneethasagari, D Pradeep, E Naga Chaithanya, D Pavani, D V Sai Sudheer, "A New Video Compression Method using DCT/DWT and SPIHT based on Accordion Representation", I.J. Image, Graphics and Signal Processing, pp. 28-34, May 2012.

[15] Jaya Krishna Sunkara, Purnima Kuruma, Ravi Sankaraiah Y, "Image Compression Using Hand Designed and Lifting Based Wavelet Transforms", International Journal of Electronics Communications and Computer Technology, vol. 2 (4), 2012.

[16] Dr. G.A.E. Satish Kumar, Jaya Krishna Sunkara, "Multiresolution SVD based Image Fusion", IOSR Journal of VLSI and Signal Processing, vol. 7, Issue 1, ver. 1, pp. 20-27, Jan-Feb 2017. DOI: 10.9790/4200-0701012027.

[17] V. V. Satyanarayana Tallapragada, G. V. Pradeep Kumar and Jaya Krishna Sunkara, "Wavelet Packet: A Multirate Adaptive Filter for De-noising of TDM Signal", International Conference on Electrical, Electronics, Computers, Communication, Mechanical and Computing (EECCMC), Jan 2018, Vellore.